PNAS RESEARCH ARTICLE | ECOLOGY OPEN ACCESS

Warming-induced tree growth may help offset increasing disturbance across the Canadian boreal forest

Jiejie Wang[a,1], Anthony R. Taylor[a], and Loïc D'Orangeville[a]

Edited by Sandra Lavorel, Grenoble Alpes University, Grenoble, France; received July 29, 2022; accepted November 11, 2022

Large projected increases in forest disturbance pose a major threat to future wood fiber supply and carbon sequestration in the cold-limited, Canadian boreal forest ecosystem. Given the large sensitivity of tree growth to temperature, warming-induced increases in forest productivity have the potential to reduce these threats, but research efforts to date have yielded contradictory results attributed to limited data availability, methodological biases, and regional variability in forest dynamics. Here, we apply a machine learning algorithm to an unprecedented network of over 1 million tree growth records (1958 to 2018) from 20,089 permanent sample plots distributed across both Canada and the United States, spanning a 16.5 °C climatic gradient. Fitted models were then used to project the near-term (2050 s time period) growth of the six most abundant tree species in the Canadian boreal forest. Our results reveal a large, positive effect of increasing thermal energy on tree growth for most of the target species, leading to 20.5 to 22.7% projected gains in growth with climate change under RCP 4.5 and 8.5. The magnitude of these gains, which peak in the colder and wetter regions of the boreal forest, suggests that warming-induced growth increases should no longer be considered marginal but may in fact significantly offset some of the negative impacts of projected increases in drought and wildfire on wood supply and carbon sequestration and have major implications on ecological forecasts and the global economy.

climate change | forest permanent sample plots | Canadian boreal forest | gains in tree growth | forest disturbance

Significance

Warmer temperatures have the potential to increase productivity in the cold-limited, Canadian boreal forest, but evidence remains controversial. We explored the climatic sensitivity of growth of the six most abundant boreal tree species in North America using an unprecedented network of permanent sample plot records distributed across both Canada and the United States. Our results indicate an overall positive effect of warming on tree growth under several climate change scenarios by midcentury, peaking in the colder, wetter regions of the boreal forest. Despite substantial variations among regions and species, such higher growth rates may help offset some of the negative impacts of projected increases in forest disturbance on future wood supply and carbon sequestration.

The Canadian boreal forest—comprising one third of the global boreal forests and over 8% of the world's forests—is one of the few remaining intact natural biomes (1, 2). Its growth is an important regulator of global atmospheric carbon flux (3) and sustains the largest softwood lumber and newsprint industry in the world (4).

Unfortunately, Canada's boreal forest is expected to be disproportionately affected by global warming as temperatures rise faster at higher latitudes (5, 6). Future warmer, drier conditions are projected to intensify the natural fire regime, with dire consequences on the goods and services the boreal forest provides (7, 8). Current estimates suggest that growth increases of 50% or more may be necessary to offset future wood fiber and carbon losses from fire in the boreal (9–11). However, future warming may also have the potential to accelerate the productivity of the boreal forest, currently limited by its cold climate (12–14), which could help offset increases in disturbance (15). The potential benefit of enhanced growth trends remains controversial and overlooked mainly because of limited data availability, methodological biases, and regional variability in forest dynamics (13, 16–18). Indeed, large discrepancies reported between empirical tree growth observations and dynamic vegetation models suggest substantive inaccuracies in our ability to predict growth in response to climate (19–22). Yet, our capacity to anticipate the future health of the boreal forest, and its recovery from intensifying disturbances, hinges on our ability to accurately project future boreal growth.

Today, process-based, dynamic vegetation models are the standard approach to project the impacts of climate change on forest growth (22, 23). However, many are limited by overly simplistic assumptions of tree ecophysiology and population dynamics (24, 25). Notably, optimal tree growth is typically expected to occur under climates found at the center of a species geographical range, declining toward the edges. Unfortunately, this approach tends to ignore the complex, nonlinear nature of tree growth, controlled by interacting climate variables such as temperature and precipitation (16), that may be further modulated by tree size (26, 27), age (28), crown position (29), genotype (30), competition (31, 32), and soil moisture conditions (33). Consequently, more robust, empirically derived estimates of climate–growth relationships are needed to refine models and improve ecological forecasts to inform adaptive forest management strategies.

Up to now, matching annual tree-ring widths with historical climate has been the preferred approach to estimate empirical, species-specific climate–growth relationships in

Author contributions: J.W., A.R.T., and L.D. designed research; J.W., A.R.T., and L.D. performed research; J.W., A.R.T., and L.D. contributed new reagents/analytic tools; J.W., A.R.T., and L.D. analyzed data; and J.W., A.R.T., and L.D. wrote the paper.

The authors declare no competing interest.

This article is a PNAS Direct Submission.

[1]To whom correspondence may be addressed. Email: jiejie.wang@unb.ca.

This article contains supporting information online at https://www.pnas.org/lookup/suppl/doi:10.1073/pnas.2212780120/-/DCSupplemental.

Published January 3, 2023.

the boreal (17, 34, 35). However, such approaches are subject to several critical biases (36–38). The largest being missing information on past changes in forest stand conditions, referred to as the "fading record" problem, which can lead to false attribution of long-term growth changes to climate when, in fact, it may be more related to forest stand dynamics (39). Moreover, tree-ring studies unintentionally tend to sample fast-growing trees in young plots and slow-growing trees in old plots, which can mistype or exaggerate growth changes (38, 40). Only recently have researchers begun to explore an alternative approach: leveraging the broadly distributed, repeatedly measured, forest permanent sample plot (PSPs) networks that cover wide climatic gradients and the geographical ranges of most boreal tree species in North America. This novel use of "old" plot networks—initially established for forest inventory purposes—is not burdened by the same biases as tree-ring sampling (17), but no study has yet merged all major available sample plot networks from both the United States and Canada to provide a more definitive evaluation of boreal tree species climate sensitivity across their native range.

In this study, we compiled over 1 million tree growth records from 20,089 PSPs (Fig. 1*A*), covering the 1958 to 2018 time period and spanning a 16.5 °C climatic gradient distributed across both Canada and the United States to study the influence of climate on tree growth for the six most abundant boreal tree species in North America, including balsam fir (*Abies balsamea),* black spruce (*Picea mariana),* white spruce (*Picea glauca),* jack pine (*Pinus banksiana*), white birch (*Betula papyrifera*), and trembling aspen (*Populus tremuloides*). Specifically, we used a machine learning algorithm—boosted regression tree (BRT) analysis—to disentangle nonlinear and interacting climatic and CO_2 controls on tree growth while controlling for tree size, competition with neighboring trees, topography, and soil characteristics (*SI Appendix*, Table S1). Fitted, species-specific BRT models were then used to predict the future growth of the Canadian boreal forest under different climate forcing scenarios for the near-term 2050 s time period. By including growth observations in our training data that extend beyond the boreal forest into each species' warmer, southern range limits, it permitted us to simulate the growth response of most of Canada's boreal forest to projected climate change without extrapolating beyond the observed climate–growth inference space (Fig. 1*B*).

Results

Drivers of Boreal Tree Growth. The fitted BRT models had good explanatory power, with pseudo-R^2 ranging between 31.8% (white birch) and 62.5% (aspen) on the testing data (*SI Appendix*, Table S2). Model error (normalized root mean square error: NrmsE; *Materials and Methods*) remained low, ranging from 14.9% (jack pine) to 23.3% (white birch).

For each tree species, at least one of the thermal-related climate variables (i.e., maximum summer temperature: $Tmax_{summer}$; minimum winter temperature: $Tmin_{winter}$; and frost-free period: FFP; *SI Appendix*, Table S1) ranked among the three strongest predictors of growth (*SI Appendix*, Table S2). Of these, $Tmax_{summer}$ and FFP (both indicators of growing season heat availability) were

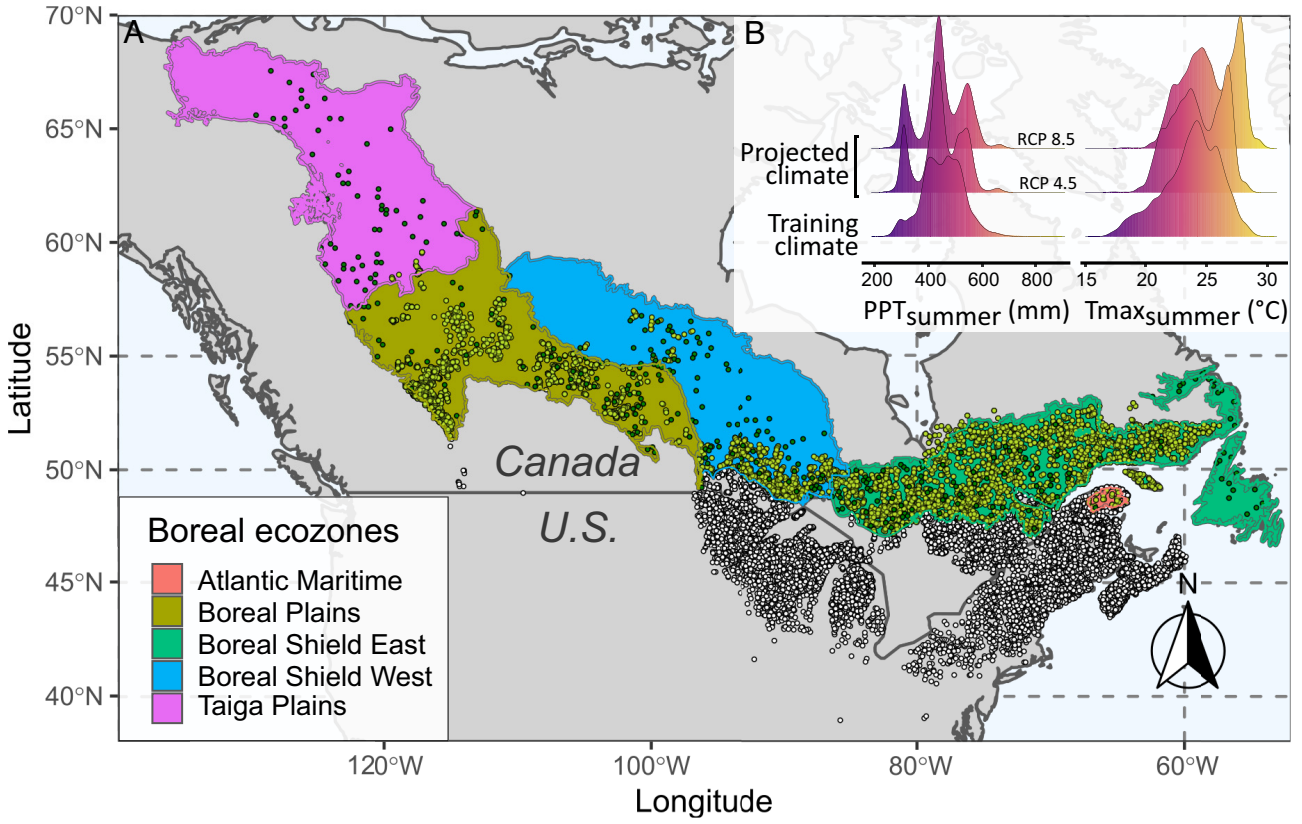

Fig. 1. Location of PSPs and distribution of their associated climate spaces. (*A*) Plots within (light green) and south (white) of the boreal forest region were used to calibrate boosted regression tree models. NFI sample plots (dark green) and boreal PSPs (light green) were used to simulate growth under projected climate. Colored regions represent the main boreal ecozones under study. (*B*) Comparison of climate spaces between the historic training climate data (including plots south of the boreal forest region) and projected climate (limited to the boreal forest region) represented as kernel density estimates of historic and future summer precipitation (PPT_{summer}) and summer temperature ($Tmax_{summer}$; *SI Appendix*, Table S1) under two radiative forcing scenarios (RCP 4.5 and 8.5) for the 2050 s time period. By including plots south of the boreal forest region in the training data, our projections mostly remained within the observed historic training data climate space, thus limiting extrapolation.

most influential, but their effect on growth varied by species (Fig. 2). White spruce, aspen, and jack pine displayed a clear temperature optimum, with large positive warming effects up to a $Tmax_{summer}$ of 23.4, 27.0, and 26.2 °C, respectively, followed by growth declines under warmer summer temperatures (Fig. 2*A*). The remaining species maintained a positive growth response to

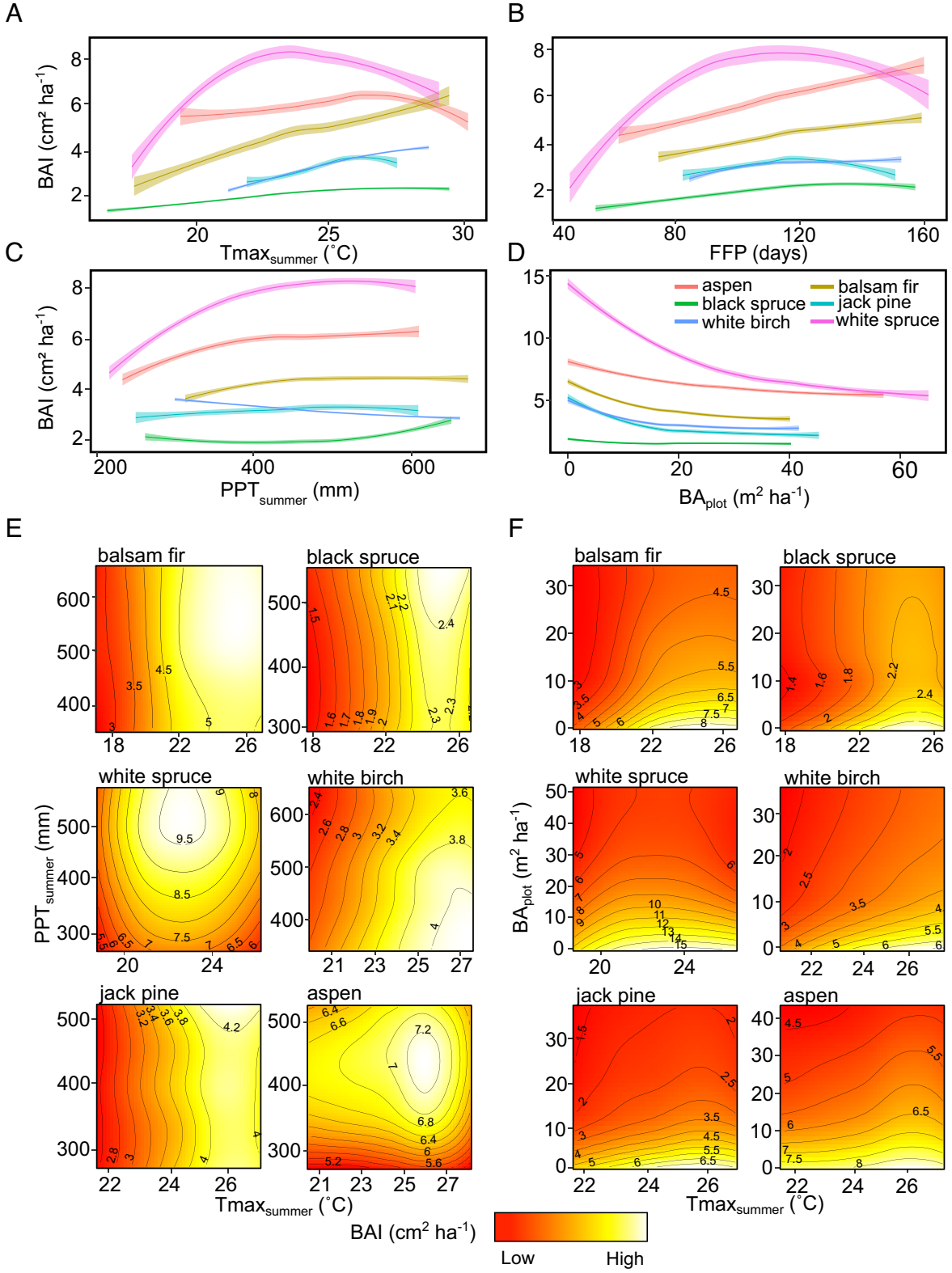

Fig. 2. Predicted growth response to climate and competition. (*A–D*) Growth response to $Tmax_{summer}$, FFP, PPT_{summer}, and BA_{plot}, respectively, across species. Curves represent smoothed partial dependence plots derived from fitted, species-specific boosted regression tree models with 95% CI. (*E*) Interactive effects of summer temperature ($Tmax_{summer}$) and precipitation (PPT_{summer}) on the growth of study species showing stronger temperature forcing on growth under higher precipitation. (*F*) Interactive effects of summer temperature ($Tmax_{summer}$) and competition (BA_{plot}) on tree growth showing stronger temperature forcing on growth under low competition. In (*E*) and (*F*), only values within the 5th to 95th quantiles of the corresponding gradients are displayed. Refer to *SI Appendix*, Table S1 for variable acronyms.

warming across all summer temperature gradients with no growth decline to warming. Winter temperature had lower relative importance (RI) values than $Tmax_{summer}$ or FFP for all species but jack pine (*SI Appendix*, Table S2), whose growth increased under warmer winter temperatures (*SI Appendix*, Fig. S1).

Except for white birch, summer precipitation had a general, positive influence on the growth of all species (Fig. 2*C*), which increased under higher temperatures, revealing a strong interaction between precipitation and temperature (Friedman's H-statistics > 0.1; Fig. 2*E*). White spruce was the most sensitive to precipitation-related variables, with large growth reductions under low PPT_{summer} gradients (mean annual basal area increment: BAI of 8 $cm^2 \cdot y^{-1}$ when PPT_{summer} >400 mm to 4.7 $cm^2 \cdot y^{-1}$ when PPT_{summer} < 210 mm). Moreover, its large growth decline under high temperatures was only marginally offset by higher precipitation (Fig. 2*E*). Aspen displayed a continuous, positive response to increasing PPT_{summer} (Fig. 2*C*), which was strongest under higher temperatures ($Tmax_{summer}$ above 25 °C; Fig. 2*E*). Jack pine displayed the weakest interaction between temperature and precipitation. Precipitation as snow (PPT_{snow}) displayed higher RI scores than PPT_{summer} for all species but aspen. However, PPT_{snow} impacts on growth were inconsistent across species (*SI Appendix*, Fig. S1). Jack pine displayed a clear PPT_{snow} optimum, with growth peaking under 260 mm of snow, while other species displayed positive (balsam fir, black spruce, white birch, and aspen) or negative (white spruce) responses with increasing snow levels.

Tree size (i.e. BA_{tree}) was the strongest predictor of growth in all species models and displayed a positive, linear effect on growth for all species (*SI Appendix*, Table S2 and Fig. S1). Interestingly, its effect varied with temperature, where larger trees displayed stronger warming gains in growth relative to smaller trees (*SI Appendix*, Fig. S2 and Text S1). Stand-level competition (BA_{plot}) was the 3rd most important model predictor across species and had a consistently, strong suppressing effect on tree growth (Fig. 2*D*). Competition levels also affected temperature responses as positive warming effects were overall stronger under conditions of low competition (Fig. 2*F* and *SI Appendix*, Text S1).

For all species but black spruce, site conditions (i.e., slope, aspect, and soil moisture regime) had only minor influence on growth, with overall low RI scores (0.0 to 6.1, ranking between 4th and 11th; *SI Appendix*, Table S2). Similar to other species, black spruce displayed lower growth on hydric soils (*SI Appendix*, Fig. S1), but soil moisture regime had a stronger influence on black spruce growth (RI = 18.4) relative to other species (*SI Appendix*, Table S2). The high RI of soil moisture regime on black spruce growth is likely due to the greater prevalence of black spruce in wetlands relative to other species. For example, in Ontario, Canada, black spruce made up 96% of study trees found in wetlands (within the hydric soil moisture class).

The impact of atmospheric CO_2 concentration on growth was relatively low with small RI scores across species, ranking between 3rd (aspen) and 10th (black spruce; *SI Appendix*, Table S2). Aspen and balsam fir showed the strongest CO_2 fertilization effects, while black spruce and jack pine showed the least effects (*SI Appendix*, Fig. S1). White spruce displayed a marginal CO_2 optimum, with positive effects up to a CO_2 concentration of 372 ppm.

Projected Growth under Climate Change. When the fitted BRT models were applied to future climate projections, we observed an average increase of 20.5 to 22.7% in the mean plot-level growth of all studied species over the next 30 y (for the 2050 s time period) across the five boreal forest ecozones under RCP 4.5 and 8.5. Due to similarity in projected responses between the two climate forcing scenarios, hereafter we focus only on results from RCP 4.5.

The large overall positive growth responses reported here varied substantially among regions. The eastern Canadian boreal region displayed the highest gains in growth, with a projected 26.2% increase in growth over the Boreal Shield East ecozone for the 2050 s driven by the high abundance of black spruce, balsam fir, and jack pine (Fig. 3). One exception was the boreal portion of

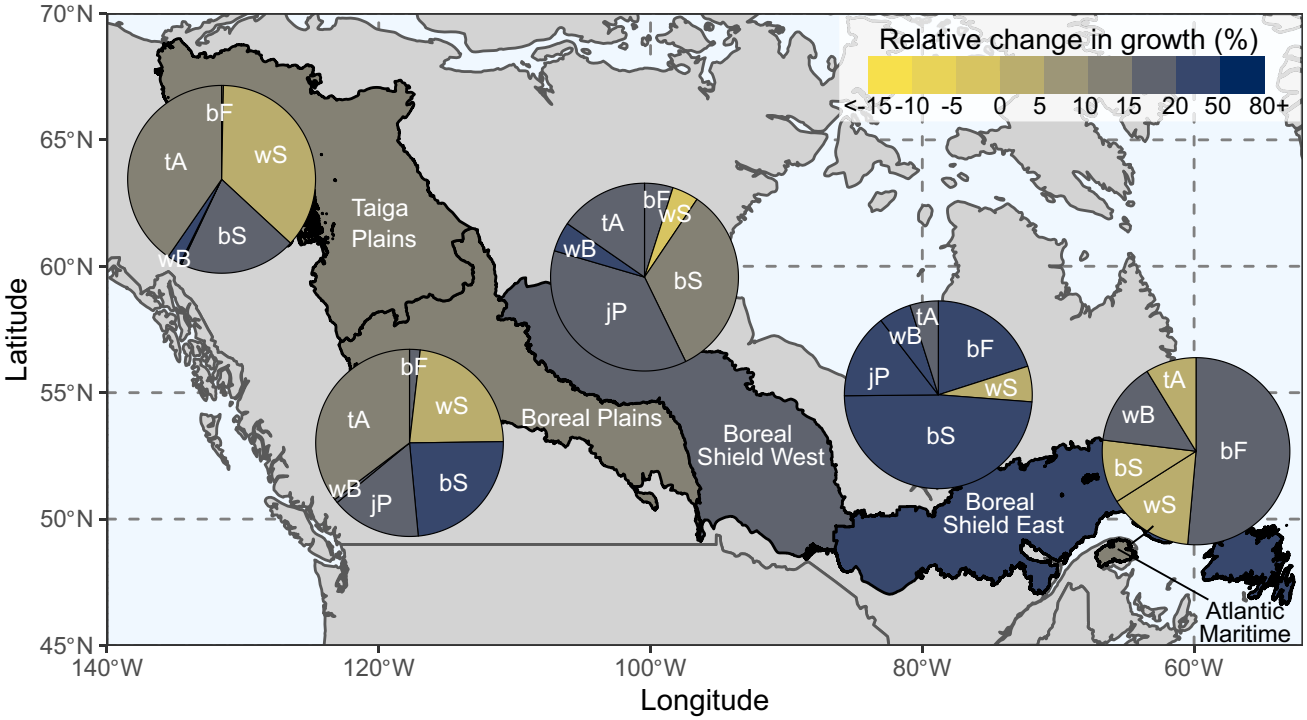

Fig. 3. Relative change in growth projected for each Canadian boreal forest ecozone under radiative forcing scenario RCP 4.5 for the 2050 s time period. The pie charts indicate the relative contribution of each species to the overall change per ecozone based on the relative total basal area per species. bS: black spruce; bF; balsam fir; jP: jack pine; wS: white spruce; wB: white birch; tA: trembling aspen.

the Atlantic Maritime ecozone, projected to have the lowest growth gains of 10.7%, likely associated with the relatively warmer and wetter baseline climate condition and lower projected warming. In Central Canada, the Boreal Plains and Boreal Shield West ecozones displayed moderate gains of 13.4 and 17.7%, respectively, driven by growth increases from black spruce (in the Boreal Plains) and jack pine and aspen (in the Boreal Shield West; Fig. 3). The net gain in growth in the Boreal Plains was reduced by the poor performance of white spruce in the region. Finally, growth in the high-latitude, westernmost Taiga Plains ecozone was projected to increase by more than 14.1% on average due to moderate increases in black spruce and aspen growth and declines in white spruce growth (Fig. 3).

These growth trends across ecozones are due, in part, to species-specific performances under baseline and future climate conditions (Fig. 4). Across all boreal ecozones, white birch (median ± SD, 20.7 ± 16.4%) displayed the highest median gains in growth under RCP 4.5, relative to baseline climate, followed by black spruce (18.7 ± 18.7%), jack pine (18.7 ± 31.7%), aspen (16.6 ± 8.9%), balsam fir (15.4 ± 13.8%), and white spruce (−1.2 ± 13.8%). Still, species responses varied spatially within ecozones (at the ecodistrict level) and across ecozones. In the eastern boreal region (east of 80°W), all species were projected to accelerate their growth by 0.6 ± 15% (white spruce) to 42.9 ± 41.1% (jack pine; Fig. 4). In the same region, growth increases were maximal north of 50°N, with larger gains of 41.0 ± 17.3% (balsam fir) to 99.9 ± 23.9% (jack pine) and more moderate gains of 19.2 ± 7.3% for aspen and 24.5 ± 13.7% for white spruce (Fig. 4). In Central Canada (80 to 100°W), aspen and white birch were projected to experience moderate, homogeneous gains in growth ranging between 21.2 ± 11.6% and 22.1 ± 11.6%, respectively, while black spruce (10 ± 21.9%) and jack pine (18.5 ± 26.8%) displayed latitudinally contrasted growth responses with gains in northern cold ecodistricts and declines in warmer, drier ecodistricts within the Boreal Shield West ecozone and the western portion of the Boreal Shield East ecozone (Fig. 4). On the contrary, no significant change in median white spruce growth was expected (−3.4 ± 7%) in the central region, despite some localized growth declines up to 60%. Similar trends were observed in western regions (west of 100°W), although several species displayed marginal growth anomalies in ecodistricts bordering the Rocky Mountains within the Taiga Plains and Boreal Plains ecozones (Fig. 4).

Discussion

The results presented in this study confirm the strong role of temperature and water availability as drivers of boreal tree growth. The overall large, positive relationship between thermal energy (warmer but also longer growing season) and growth supports earlier findings from controlled experiments (41, 42), remote sensing observations (14, 18), tree-ring analyses (12), and forest inventory approaches (43, 44). Temperature is critical to many biochemical processes such as photosynthesis, which can benefit from warming in cold ecosystems due to quicker enzymatic functions, leading to higher carbon assimilation (41). Additionally, warming-induced lengthening of the growing season expands the growing period and allows earlier leaf flush in deciduous species, which can stimulate carbon sequestration (45). Here, in the cold-limited, boreal forest, climate warming is likely to promote C assimilation, nutrient uptake, and C sequestration, leading to greater radial growth (6, 18, 46, 47). Furthermore, rising atmospheric CO_2 concentration under climate change could also enhance photosynthetic rate and water use efficiency due to CO_2 fertilization effects (41, 48). However, our analysis also highlights the strong control of local water availability on the growth trajectory of boreal trees in response to warming, consistent with previous research from in situ experiments (33), tree-ring analyses (16, 34, 49, 50), forest inventory approaches (51, 52), and remote sensing observation (14, 53). Warming-induced increases in atmospheric vapor pressure deficit can inhibit photosynthesis and carbon uptake, with higher risks of carbon starvation and hydraulic failure due to decline in stomatal conductance (54–56). Similarly, increases in temperature-induced evaporation may cause water stress, reductions in turgor pressure, stomatal closure, and decline in photosynthesis and carbon uptake (33, 57). This warming-induced water stress, along with increasing respiration cost, has been reported to dampen tree growth and increase risks of tree mortality in different regions (58–61).

The overall gains in growth projected here for most of the Canadian boreal forest, with the largest growth increases projected for the eastern, wetter region, are in line with recent observations of positive growth trends in boreal and temperate forests (13, 14, 18, 35, 43, 44, 62, 63), as well as earlier growth projections from empirical (16) and modeling approaches (20, 22), but contradict other studies (64–67). Such divergences may be due to certain limitations inherent to the approaches used to confront this complex issue. Process-based, dynamic vegetation models rely heavily on leaf-level processes (24, 25), which tend to produce substantive inaccuracies in predicting tree growth responses to climate (22), while growth projections from tree-ring data tend to confound historical forest stand development processes with climate effects on growth (36–40). Here, despite their coarser time resolution and higher cost in data acquisition, well-replicated PSPs offer an exhaustive, more accurate portrait of climatic regulation on boreal tree growth.

Within our overall projection of growth enhancement across the boreal forest, large discrepancies were observed among regions which tracked local variations in hydroclimate and species composition (6, 13, 18). The projected trend of greater gains in growth at higher latitudes, in line with previous research, is likely caused by the stronger current thermal limitation on growth in colder boreal regions combined with higher projected rates of climate warming (16, 53, 68). We also report a longitudinal trend in growth responses, where wetter eastern ecozones displayed the largest growth gains and drier, central ecozones the least, including marginal declines, suggesting drier parts of the boreal biome will become more vulnerable to growth reductions under warming (12, 14, 69, 70). The marginal decline observed in some western and southern ecodistricts is likely associated with a drier moisture balance combined with limited increases in precipitation. The reduced gains in Central and Western Canada may also be attributed in part to the higher proportion of white spruce, which is the only species studied here to display a rapid growth decline in the near term, in agreement with multiple empirical studies (16, 71, 72). White spruce growth decline has been repeatedly associated with high temperatures in excess of the species physiological thresholds (73, 74). Among the six species studied here, white spruce also displayed the highest sensitivity to low water availability, in line with recent reports of drought-induced growth decline, and even mortality in Central and Western Canada for that species (71, 72, 75–77).

Climate-driven increases in rates of natural disturbances are expected to have a growing impact on boreal forest wood supply and carbon storage (78). Notably, significant reductions in forest cover are projected following forest regeneration failure from successive disturbances (79–81) or combinations of disturbances (82). However, our growth projections (20.5 to 22.7% increase on average across Canada's boreal ecozones) are much higher than

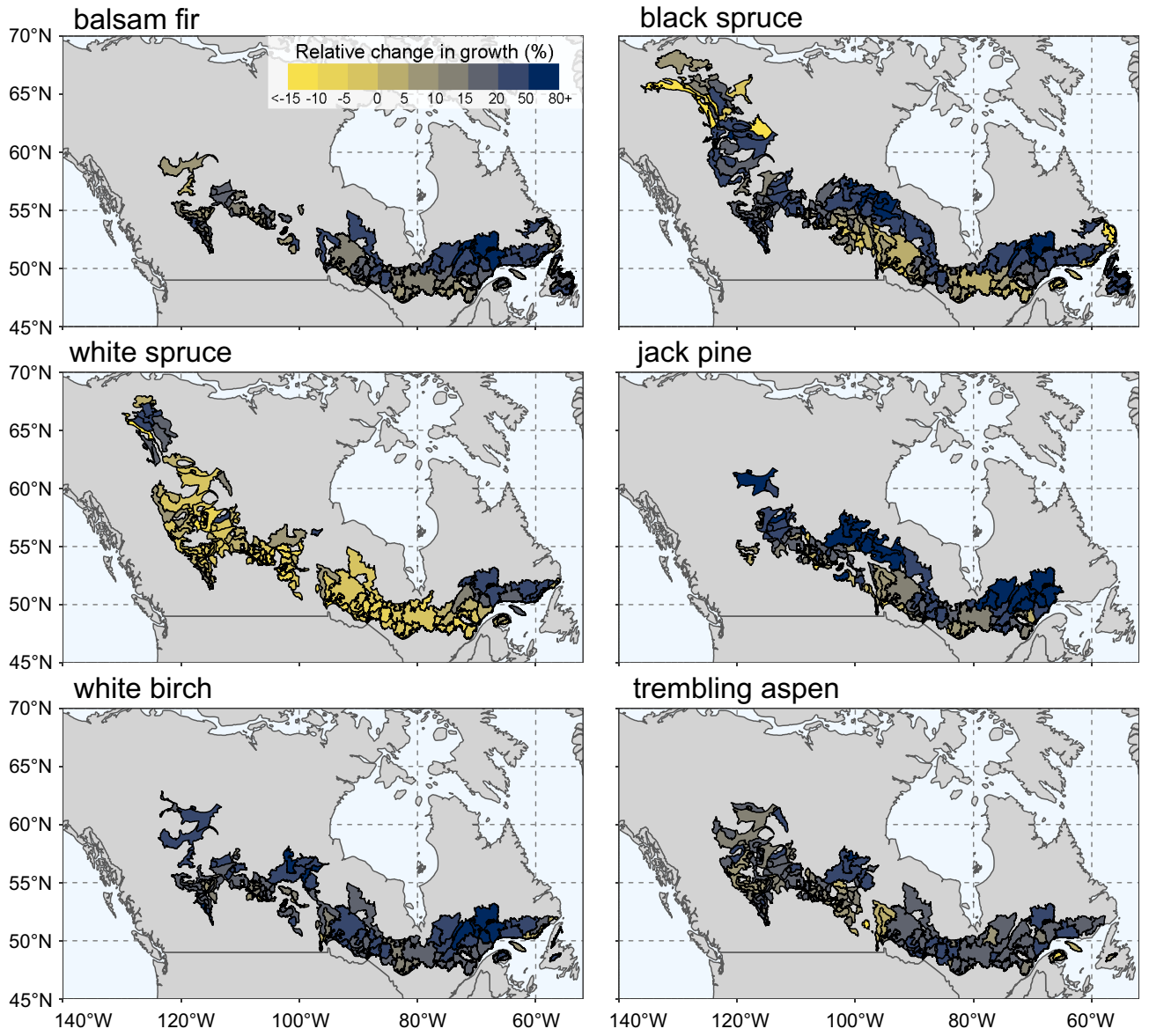

Fig. 4. Relative change in tree growth projected for the six study species in each Canadian boreal forest ecodistrict under radiative forcing scenario RCP 4.5 for the 2050 s time period.

reported by previous studies (16, 65) and suggest that future growth increases may help offset wood fiber and carbon losses from increasing fire in the boreal forest (9–11), especially in Eastern Canada (83). The acceleration of growth in black spruce, jack pine, and aspen reported here is particularly noteworthy given these species have been identified as most vulnerable to future intensification of drought in south central Canada (aspen) and fire in central and eastern Canada (black spruce and jack pine) (83). Even so, our projections should be interpreted carefully as they do not include future changes in forest properties such as composition, age, disturbance rates, or account for genetic variations within species across their geographic range, which can influence forest-level responses to climate change (6, 28, 30, 83). We also emphasize that growth is but one of several processes, such as recruitment and mortality, that drive forest-level productivity and demographics and therefore must be interpreted accordingly. However, some of the plots which we excluded from our analysis due to excessive mortality could have suffered severe climatic anomalies such as the 2001 to 2002 drought in central Canada (84), leading to potential underestimation of their impact on growth. Such events are important catalysts of forest type transitions but were relatively rare (less than 1% of sites from all PSPs we collected were excluded due to excess mortality), and species-specific growth rates remain a critical predictor of postdisturbance recovery (85). Lastly, it is critical the empirically derived estimates of climate–growth relationships presented here be used to benchmark and parameterize process-based, dynamic vegetation models to help improve ecological forecasts and inform adaptive management strategies (86). Overall, our results suggest that the effects of climate change on boreal forest growth, especially in eastern regions, may have major ramifications on future wood fiber supply, carbon storage, and the global economy.

Materials and Methods

Study Area. Our study spans a wide environmental gradient, mainly encompassing the boreal and northern temperate forests of eastern and central North America (Fig. 1*A*), covering a large extent of the geographical range of boreal tree species.

Climate ranges from subarctic in the north, with cool, short summers and long, cold winters, to temperate in the south, with hot summers and mild winters, covering a wide gradient in the mean annual temperature (−4.9 to 11.6 °C), precipitation (350.5 to 1959.4 mm), and FFP (56.4 and 178.8 d). The boreal forest is dominated by cold-adapted tree species, such as white spruce, black spruce, balsam fir, trembling aspen, and white birch, but our study area also includes the southern range of these boreal species, where they co-occur with warmer-adapted temperate tree species such as red maple (*Acer rubrum*), yellow birch (*Betula alleghaniensis*), American beech (*Fagus grandifolia*), and eastern hemlock (*Tsuga canadensis*). In addition to management, boreal forest dynamics are driven by large-scale disturbances such as wildfires and insect outbreaks along with pathogens, wind, flooding, and ice storms, with varying intensity and frequency across regions and forest types (6).

Data and Sampling Design. We obtained forest stand and tree information from repeatedly measured PSPs distributed across eastern and central North America, including the US Forest Inventory and Analysis (FIA) program (31 eastern states), Canada's National Forest Inventory (NFI) program, and the Canadian PSP programs from the provinces of Nova Scotia, New Brunswick, Quebec, Ontario, Manitoba, Saskatchewan, and Alberta. Note that remeasurements from NFI plots were not yet available during this analysis, but these plots were used to project future growth (described later in *Materials and Methods*). All PSPs follow fixed-radius plot designs. Plot design and sampling procedures are consistent among the US FIA plots but vary across Canadian jurisdictions (87–94). Thus, for all plot measurements, we applied the following selection procedures (first at plot level and then at tree level) to standardize and compile all observations into a single, comprehensive database.

We first selected for plots with known coordinates and at least two successive measurements which contained at least one of the study species. Among these 41,518 selected plots, 33% (13,854 PSPs) were excluded due to the presence of severe natural (e.g., insects, disease, and fire) or anthropogenic (e.g., silviculture) disturbance reported during data collection. In the absence of disturbance records, we excluded another 18.2% (7,575 PSPs) with unusually high annual mortality rates above 6%·y^{-1} suggesting nonreported disturbance (*SI Appendix*, Table S3, Fig. S4, and Text S2) (95–98). These selection criteria resulted in 20,089 repeatedly measured PSPs remaining for further analysis, including 611,554 individual trees. To avoid trees with growth limited by nonclimatic factors (29), we excluded damaged and suppressed trees. First, we excluded 52,760 individual trees (8.6% of total) from the remaining 20,089 plots that displayed significant damage based on field crew records. Suppressed trees needed to be identified based on their canopy position. A portion of missing canopy position data in each jurisdiction (overall 26.1% missing information from initial tree records) led us to compute for each tree the basal area of larger trees (BAL; the sum of basal area of trees larger than the target tree), where dominant trees tend to display low BAL values (99). In plots with known canopy position, 75% of dominant–codominant trees displayed BAL ≤ 17.4 m^2·ha^{-1}. To exclude suppressed trees, we excluded all trees in all plots with BAL values above that threshold, representing 100,128 individual trees, or 16.4% of trees in selected plots. Separate analyses including suppressed trees yielded very similar results (*SI Appendix*, Table S4 and Text S3). This selection procedure retained 20,089 repeatedly measured PSPs and 458,666 individual trees for a total of 1,242,108 tree measurements (1958 to 2018) for further analysis. The selected PSPs are well distributed among all forested ecozones in Canada's boreal forest east of the Rockies from the cool and wet Atlantic Maritime ecozone to the cold and semiarid Taiga Plains ecozone (Fig. 1*A*).

Tree Growth. Annual basal area increment (BAI, cm^2·y^{-1}) is considered an important indicator of tree species performance and commonly used to quantify tree growth in boreal forests (16, 69). The BAI of each individual tree was calculated as the difference in basal area between two successive measurements over the time interval between plot measurements in years. Anomalous BAI values of each species were removed using Tukey's approach, where outliers were defined as values more than three times the interquartile range from the quartiles of the species-specific BAI distribution. Following this procedure, less than 3% of records of each species were removed. Alternative outlier detection methods including random sampling, visual examination, and exclusion of values outside the 95% percentile across species-specific BAI distributions had no impact on our modeling results. BAI was log-transformed (i.e., log(BAI+1)) as the response variable to avoid negative growth predictions. Back-transformed BAI estimates are presented herein by applying an exponential function.

Explanatory Variables.

Climate. Historic climate data used to train species-specific BRT models for each specific plot location and measurement interval were obtained from 1-km resolution interpolated climate grids provided by the Natural Resources Canada (100). To assess the control exerted by heat on tree growth, the mean maximum summer temperature ($Tmax_{summer}$; May to September; range: 16 to 30 °C), mean minimum winter temperature ($Tmin_{winter}$; January to March; range: −33 to −5 °C), and frost-free period (FFP; range: 45 to 179 d) were calculated since they are well correlated with tree growth during the growing season (23), restrict growth in colder environments (101, 102), and are commonly used to evaluate the impact of growing season length on growth, respectively. Species geographical distributions along the range of these variables were generally similar (*SI Appendix*, Fig. S3).

The mean summer precipitation (PPT_{summer}; May to September; range: 217 to 880 mm) and precipitation as snow (PPT_{snow}; January to March; range: 23 to 917 mm) were calculated to assess the control of water availability on growth. PPT_{summer} is a hydrologic index well correlated with growing season water availability that impacts tree growth (101). PPT_{snow} was used to account for the long-lasting effects of spring snowmelt on growing season water availability, estimated as the total snowfall from January to March. Balsam fir, white birch, and black spruce were more abundant at high PPT_{summer} (median values of 500, 486, and 454 mm, respectively) than other species (median values of 395 to 409 mm; *SI Appendix*, Table S2). Similar distribution patterns were displayed along January to March snowfall among species (*SI Appendix*, Fig. S3). Balsam fir, white birch, and black spruce were more abundant at high snow amounts (median values of 289 to 338 mm) than other species (median values of 134 to 182 mm; *SI Appendix*, Table S2). At each plot, climatic variables were averaged over the period between successive measurements (e.g., the interval between the ith and i+1th measurements) to obtain interval-specific climate estimates. Climate moisture index (CMI), an index of atmospheric moisture balance calculated from the difference between precipitation and potential evapotranspiration, is well correlated with tree growth in boreal and temperate forest ecosystems (57, 103). Here, the replacement of PPT_{summer} with CMI led to minimal differences in the BRT model results for each species (*SI Appendix*, Table S5, Fig. S5, and Text S4), likely due to the high correlation (Pearson's correlation = 0.85) between these variables.

CO_2. Elevated atmospheric CO_2 can directly enhance growth due to CO_2 fertilization effects and increase water use efficiency (48, 104, 105). Given the collected tree growth records span over the past six decades, we assumed that significant variation in CO_2 might affect our models. Historic global CO_2 data were obtained from the Earth System Research Laboratories (gml.noaa.gov/ccgg/trends/). Global CO_2 has increased by approximately 100 ppm over the past six decades (from 316 ppm in 1960 to 416 ppm in 2021). To obtain interval-specific CO_2 estimates for each plot, we averaged historic CO_2 (in ppm) over the period between successive measurements of each plot. Atmospheric CO_2 concentration levels and their distribution were similar across species, with median values ranging between 353 (white spruce) and 377 ppm (balsam fir; *SI Appendix*, Table S2).

Stand Characteristics. Slope inclination and aspect, which influence the amount of solar radiation reaching the forests, were calculated from a 1-arc-second (approximately 30 m) resolution digital elevation model provided by the US Geological Survey (https://viewer.nationalmap.gov/basic/) for the Canadian PSPs but derived from actual plot records for the US FIA plots. All calculations were completed in R (106) using the raster package (107). The majority of plots were located on relatively flat-sloped landscapes (median value of 2% and 95th percentile of 16%; *SI Appendix*, Fig. S3). Aspect was determined as a continuous variable and then transformed as one of three categories: 1) SE-SW (corresponding to the warm aspect), 2) NW-NE and flat (cold aspect), and 3) SE-NE and SW-NW (moderate aspect). All tree species were most abundant on moderate versus cold or warm aspects (*SI Appendix*, Fig. S3).

Soil moisture regime can have strong effects on nutrient availability, root distribution, and photosynthesis rate and thus mediate tree growth (33, 103). We derived an index of the local soil moisture regime for each PSP using physiographic class (US PSPs) or from plot field observations of soil moisture and/or drainage, texture, and organic matter composition (Canadian PSPs). Records of soil moisture regime from all PSPs were standardized and transformed into one of three categories: 1) xeric (dry site), 2) mesic, and 3) hydric (wet site). Species were most common on mesic sites, except jack pine, which was more frequent

on xeric sites (63% of sampled jack pine trees) and black spruce, which was more common on hydric sites than other species (*SI Appendix*, Fig. S3).

Competition (BA_{plot}). Although our analysis was limited to dominant and codominant trees, we calculated a plot-level competition index (BA_{plot}) to account for competition for resources from neighboring trees. For each plot and corresponding measurement, BA_{plot} was computed as the sum of all individual basal areas for trees with a diameter at breast height (1.3 m, DBH) ≥ 9 cm, scaled to a hectare (units of $m^2 \cdot ha^{-1}$). Competition levels and their distribution were similar across species, with median BA_{plot} values ranging between 17.7 (black spruce) and 28.4 $m^2 \cdot ha^{-1}$ (white spruce; *SI Appendix*, Table S2).

Tree Size (BA_{tree}). Tree basal area (BA_{tree}, referred to hereafter as tree size, calculated from DBH at 1.3 m) was used to control for tree size effects on growth. Tree size is highly correlated with tree growth and mediates climate–growth relations (27). The distribution of BA_{tree} was similar across all sampled species (*SI Appendix*, Fig. S3), although white spruce tended to be larger (median values of 438 cm^2) than other species (median values extending from 127 to 285 cm^2; *SI Appendix*, Table S2).

Model Fitting and Performance. To investigate the effects of climate and CO_2 on tree growth while controlling for endogenous (e.g., tree size) and site-level conditions (e.g., plant competition, soil moisture regime, slope, and aspect), we employed BRT analysis. BRT analysis is a machine learning, ensemble modeling method in which many simple regression trees, generated using recursive binary splits based on the explanatory power of a single variable (or predictor) at each split, are fitted in a stepwise manner (108). BRT analysis accommodates many of the violations of conventional, parametric statistics (e.g., multiple linear regression) that are common to ecological data, including missing data, departures from normality and homogeneity of variance, and strong collinearity among explanatory variables (108). While BRT has been shown to outperform other tree-based machine learning methods in predictive performance tests (109), we did try other machine learning approaches, including the random forest algorithm, but found minimal differences and chose to focus on BRT analysis to reduce complexity and ease interpretation of models.

All BRT models were fitted using the R gbm package (110). Individual BRT models were fitted for each tree species to uncover species-specific climate and CO_2 controls on growth. To produce unbiased estimates of model performance, the data were split into training (80% of initial data) and test sets (remaining 20%). We used log(BAI+1) as the response variable assuming a Gaussian distribution. The species-specific BRT models were first "tuned" by searching the optimum combination of model hyperparameters, including learning rate (shrinkage: 0.001, 0.05, and 0.1), number of trees (n.trees: 1,000 to 6,000), maximum depth of each tree (interaction.depth: 2 to 5), and minimum number of observations in the terminal nodes of trees (n.minobsinnode: 5 and 10). Hyperparameter tuning was carried out using 10-fold cross-validation on the training set using the "caret" package in R (*SI Appendix*, Table S6) (111).

The performance of the final species-specific BRT models was assessed using pseudo-R^2 and normalized rms error (NrmsE) metrics, calculated as the square of the correlation coefficient between the observed and predicted values of the response variable, and the ratio of root mean square error to the mean of corresponding response variable for each species. Relationships between the explanatory variables and response were quantified using variable RI scores. Variable RI is estimated from the number of times a variable is selected to split a tree and the improvement of this split and measures the relative influence of each explanatory variable on the response variable using a 0 to 100 scale (108). Unlike conventional regression models, BRT does not provide "coefficients" and associated uncertainty measures; therefore, there are no *P* values to indicate the statistical significance of model coefficients (108).

We used smoothed partial dependence plots (PDPs) to visualize the relationships between the explanatory variables and growth (i.e., BAI) using the "pdp" package (112) and LOESS smoothing function in R. PDPs represent the effect of an explanatory variable on growth while keeping all other explanatory variables constant at their median level (112). In addition, two-way interactions were tested for a subset of variables based on their known interactive effects (e.g., temperature and precipitation, climate and BA_{plot}, and climate and tree size). The strength of interactive effects was computed using Friedman's H-statistic ranging between 0 and 1, with larger values indicating greater interaction (113). There is currently no universally agreed-upon value of H-statistic that signifies significant interaction; therefore, we chose to investigate any 2-way interactions that resulted in an H-statistic > 0.1.

Species-Specific BRT Growth Model Format. A single BRT model was fitted for each target species to predict annual BAI of an individual tree as a function of temperature, length of FFP, precipitation, competition, tree size, stand slope and aspect, soil moisture index, and carbon dioxide concentration. A description of the response and explanatory variables can be found in *SI Appendix*, Table S1.

$$\begin{aligned}\log(\mathrm{BAI}+1) \sim\ & \mathrm{Tmax}_{summer} + \mathrm{Tmin}_{winter} + \mathrm{FFP} \\ & + \mathrm{PPT}_{summer} + \mathrm{PPT}_{snow} + \mathrm{BA}_{plot} + \mathrm{BA}_{tree} + \mathrm{Slope} \\ & + \mathrm{Aspect} + \mathrm{Soil\ moisture\ regime} + \mathrm{CO}_2. \end{aligned} \quad [1]$$

Simulated Growth under Future Climate. To predict the future growth of Canada's boreal forest under different climate change scenarios for the near-term 2050 s time period (2041 to 2070), 1-km resolution baseline climate normals data and time series climate projection data were obtained from the Natural Resources Canada (100). The baseline climate normals data were obtained by averaging historic climate over the decades 1981 to 2010. Climate projections are model ensembles averaged from five Earth System Models using monthly data downloaded from the World Climate Research Program Climate Model Intercomparison Project Phase 5 archive for two different radiative forcing scenarios, i.e., Representative Concentration Pathway (RCP) 4.5 and 8.5 (114). RCP 4.5 represents a stabilization scenario in which radiative forcing stabilizes shortly after 2100, without overshooting the 4.5 $W \cdot m^{-2}$ radiative forcing target level, while RCP 8.5 leads to radiative forcing of 8.5 $W \cdot m^{-2}$ by 2100 and continues to increase for some time afterward. Climate projections for the 2050 s time period were obtained by averaging the time series climate projection data over three decades (2041 to 2070). The five Earth System Models averaged were HadGEM2-ES, CESM1-CAM5, MIROC-ESM, CanESM2, and CCSM4, all of which produce a relatively consistent projection of climate variables across the Canadian boreal forests for 2041 to 2070 under RCP 4.5. For temperature, CanESM2 projects relatively higher median summer maximum temperatures ($Tmax_{summer}$, 26.8 °C) than the other four models, which range between 24.5 °C (MIROC-ESM) and 25.2 °C (HadGEM2-ES), while the summer precipitation (PPT_{summer}) ranges from 414 mm (HadGEM2-ES) to 437 mm (MIROC-ESM) across all models (*SI Appendix*, Fig. S6). However, climate models project a faster rate of warming at higher latitudes along with potential increases in precipitation in eastern North America under climate change (*SI Appendix*, Fig. S7). The baseline atmospheric CO_2 concentration was obtained by averaging historic global atmospheric CO_2 over three decades (1981 to 2010). The atmospheric CO_2 for the 2050 s time period was calculated by averaging the CO_2 projection values over 2041 to 2070 under RCP 4.5 and 8.5 (available at RCP Database–International Institute for Applied Systems Analysis).

We simulated future growth (BAI, $cm^2 \cdot y^{-1}$) of the study species within the five ecozones of Canada that encompass most of the boreal forest east of the Rocky Mountains, including the Taiga Plains, Boreal Plains, Western Boreal Shield, Eastern Boreal Shield, and Atlantic Maritime ecozones (115). To do so, we combined the tree lists from the most recent PSPs and NFI plots, excluding suppressed and damaged trees (Fig. 1*A*). We then simulated the growth of each individual stem using the fitted, species-specific BRT models under baseline (1981 to 2010 climate normals) and projected climate conditions of both RCP 4.5 and 8.5 for the near term (2050 s time period). For these simulations, only climate variables and CO_2 were permitted to vary according to different climate forcing scenarios (baseline climate normals, RCP 4.5 and 8.5 in 2050 s), while all nonclimatic variables (i.e., competition, tree size, soil moisture regime, slope, and aspect) were kept constant. Individual tree growth estimates were summed per plot and then scaled per hectare. Relative growth change under each climate change scenario was calculated at the plot-level relative to baseline climate conditions, then averaged per ecodistrict, which are ecologically homogeneous spatial units of 78 × 78-km area on average (115, 116). Finally, the average change in growth per species was calculated as the mean in relative growth changes across all ecodistricts for the five studied ecozones. The average change in growth across species was calculated similarly, this time combining projected growth changes for all study species in each study plot.

Simulating growth responses outside the observed climate range of the training climate data can introduce model bias and uncertainty (117). To help counter this problem, our training data included growth observations across each species' southern geographic range, well beyond the southern boundary of the boreal forest. At least four out of the total six projected climatic variables and CO_2 under each climate change scenario remained within the range of the historic observed climate and CO_2 data used to train the BRT models for each species, thus minimizing extrapolation (Fig. 1*B*).

Data, Materials, and Software Availability. Data were analyzed in the open source statistical software R (version 4.0), and the source code used to fit the growth models and project growth trends is available at https://github.com/Jiejie-Wang/boreal-forest-growth-models. The PSP information from the United States and Quebec (Canada) is public and available online at https://www.fia.fs.usda.gov/ (the United States) and https://open.canada.ca/data/en/dataset/adb12ba6-4e55-4e4a-8a63-235c48be7865 (Quebec). The PSP datasets from the remaining Canadian provinces (NS, NB, ON, MB, SK, and AB) used in this study were used under license but will be made available from the authors upon reasonable request and approval by the corresponding authorities.

ACKNOWLEDGMENTS. We thank Chris Hennigar for assistance during the preliminary steps of data cleaning and Sarah Endicott for compiling some of the climate and biophysical data. We thank the US FIA program, Canada's NFI program, and the PSP programs of the Canadian provinces of Nova Scotia, New Brunswick, Quebec, Ontario, Manitoba, Saskatchewan, and Alberta. This research was financially supported by the Natural Resources Canada–Canadian Forest Service, the New Brunswick Department of Natural Resources and Energy Development, the Natural Sciences and Engineering Research Council of Canada (Discovery Grant awarded to L.D'O.; RGPIN-2019-04353), and New Brunswick Innovation Fund (Start-up Grant; RIF 2019-029).

Author affiliations: [a]Faculty of Forestry and Environmental Management, University of New Brunswick, Fredericton E3B 5A3, Canada

1. J. P. Brandt, M. D. Flannigan, D. G. Maynard, I. D. Thompson, W. J. A. Volney, An introduction to Canada's boreal zone: Ecosystem processes, health, sustainability, and environmental issues1. *Environ. Rev.* **21**, 207–226 (2013).
2. Y. Pan, R. A. Birdsey, O. L. Phillips, R. B. Jackson, The structure, distribution, and biomass of the world's forests. *Annu. Rev. Ecol. Evol. Syst.* **44**, 593–622 (2013).
3. Y. Pan, R. A. Birdsey, J. Fang, R. Houghton, P. E. Kauppi, A large and persistent carbon sink in the world's forests. *Science.* **333**, 988–993 (2011).
4. FAO, Global forest resources assessment–2020 key findings (FAO, Rome, 2020), 10.4060/ca8753en.
5. F. J. Doblas-Reyes, A. A. Sörensson, M. Almazroui, A. Dosio, "Linking global to regional climate change" in *Climate Change 2021: The Physical Science Basis. Contribution of Working Group I to the Sixth Assessment Report of the Intergovernmental Panel on Climate Change*, V. P. Masson-Delmotte *et al.*, Eds. (Cambridge University Press, 2021).
6. D. T. Price *et al.*, Anticipating the consequences of climate change for Canada's boreal forest ecosystems. *Environ. Rev.* **21**, 322–365 (2013).
7. A. R. Taylor *et al.*, A review of natural disturbances to inform implementation of ecological forestry in nova scotia, canada. *Environ. Rev.* **28**, 387–414 (2020).
8. R. Seidl *et al.*, Forest disturbances under climate change. *Nat. Clim. Change* **7**, 395–402 (2017).
9. S. Gauthier *et al.*, Vulnerability of timber supply to projected changes in fire regime in Canada's managed forests. *Can. J. For. Res.* **45**, 1439–1447 (2015).
10. W. A. Kurz *et al.*, Carbon in Canada's boreal forest – A synthesis. *Environ. Rev.* **21**, 260–292 (2013).
11. A. F. J. Brecka *et al.*, Sustainability of Canada's forestry sector may be compromised by impending climate change. *For. Ecol. Manage.* **474**, 118352 (2020).
12. L. D'Orangeville, Northeastern North America as a potential refugium for boreal forests in a warming climate. *Science.* **352**, 1452–1455 (2016).
13. C. Loehle, K. A. Solarik, Forest growth trends in Canada. *For. Chron.* **95**, 183–195 (2019).
14. D. Sulla-Menashe, C. E. Woodcock, M. A. Friedl, Canadian boreal forest greening and browning trends: An analysis of biogeographic patterns and the relative roles of disturbance versus climate drivers. *Environ. Res. Lett.* **13**, 014007 (2018).
15. W. A. Kurz, G. Stinson, G. Rampley, Could increased boreal forest ecosystem productivity offset carbon losses from increased disturbances? *Philos. Trans. R. Soc. B Biol. Sci.* **363**, 2261–2269 (2008).
16. L. D'Orangeville *et al.*, Beneficial effects of climate warming on boreal tree growth may be transitory. *Nat. Commun.* **9**, 1–10 (2018).
17. W. Marchand *et al.*, Untangling methodological and scale considerations in growth and productivity trend estimates of Canada's forests. *Environ. Res. Lett.* **13**, 093001 (2018).
18. C. Boisvenue, S. W. Running, Impacts of climate change on natural forest productivity–Evidence since the middle of the 20th century. *Glob. Chang. Biol.* **12**, 862–882 (2006).
19. F. Babst *et al.*, Site- and species-specific responses of forest growth to climate across the European continent. *Glob. Ecol. Biogeogr.* **22**, 706–717 (2013).
20. M. P. Girardin, F. Raulier, P. Y. Bernier, J. C. Tardif, Response of tree growth to a changing climate in boreal central Canada: A comparison of empirical, process-based, and hybrid modelling approaches. *Ecol. Model.* **213**, 209–228 (2008).
21. C. R. Rollinson *et al.*, Emergent climate and CO2 sensitivities of net primary productivity in ecosystem models do not agree with empirical data in temperate forests of eastern North America. *Glob. Change Biol.* **23**, 2755–2767 (2017).
22. S. Tei *et al.*, Tree-ring analysis and modeling approaches yield contrary response of circumboreal forest productivity to climate change. *Glob. Change Biol.* **23**, 5179–5188 (2017).
23. Z. Zhang *et al.*, Converging climate sensitivities of European forests between observed radial tree growth and vegetation models. *Ecosystems* **21**, 410–425 (2018).
24. S. Fatichi, S. Leuzinger, C. Körner, Moving beyond photosynthesis: From carbon source to sink-driven vegetation modeling. *New Phytol.* **201**, 1086–1095 (2014).
25. C. Pappas, S. Fatichi, S. Leuzinger, A. Wolf, P. Burlando, Sensitivity analysis of a process-based ecosystem model: Pinpointing parameterization and structural issues. *J. Geophys. Res. Biogeosci.* **118**, 505–528 (2013).
26. M. Trouillier *et al.*, Size matters–A comparison of three methods to assess age- and size-dependent climate sensitivity of trees. *Trees Struct. Funct.* **33**, 183–192 (2019).
27. P. Mérian, F. Lebourgeois, Size-mediated climate-growth relationships in temperate forests: A multi-species analysis. *For. Ecol. Manage.* **261**, 1382–1391 (2011).
28. H. Y. H. Chen, Y. Luo, P. B. Reich, E. B. Searle, S. R. Biswas, Climate change-associated trends in net biomass change are age dependent in western boreal forests of Canada. *Ecol. Lett.* **19**, 1150–1158 (2016).
29. C. R. Rollinson *et al.*, Climate sensitivity of understory trees differs from overstory trees in temperate mesic forests. *Ecology* **102**, 1–11 (2021).
30. F. Valladares *et al.*, The effects of phenotypic plasticity and local adaptation on forecasts of species range shifts under climate change. *Ecol. Lett.* **17**, 1351–1364 (2014).
31. A. Buechling, P. H. Martin, C. D. Canham, Climate and competition effects on tree growth in Rocky Mountain forests. *J. Ecol.* **105**, 1636–1647 (2017).
32. J. Zhang, S. Huang, F. He, Half-century evidence from western Canada shows forest dynamics are primarily driven by competition followed by climate. *Proc. Natl. Acad. Sci. U.S.A.* **112**, 4009–4014 (2015).
33. P. B. Reich *et al.*, Effects of climate warming on photosynthesis in boreal tree species depend on soil moisture. *Nature* **562**, 263–267 (2018).
34. R. D'Arrigo, R. Wilson, B. Liepert, P. Cherubini, On the "Divergence problem" in Northern Forests: A review of the tree-ring evidence and possible causes. *Glob. Planet. Change* **60**, 289–305 (2008).
35. R. A. Hember, W. A. Kurz, M. P. Girardin, Tree ring reconstructions of stemwood biomass indicate increases in the growth rate of black spruce trees across boreal forests of Canada. *J. Geophys. Res. Biogeosci.* **124**, 2460–2480 (2019).
36. F. Babst *et al.*, When tree rings go global: Challenges and opportunities for retro- and prospective insight. *Quat. Sci. Rev.* **197**, 1–20 (2018).
37. S. Klesse *et al.*, Sampling bias overestimates climate change impacts on forest growth in the southwestern United States. *Nat. Commun.* **9**, 1–9 (2018).
38. C. Nehrbass-Ahles *et al.*, The influence of sampling design on tree-ring-based quantification of forest growth. *Glob. Change Biol.* **20**, 2867–2885 (2014).
39. R. J. W. Brienen, M. Gloor, G. Ziv, Tree demography dominates long-term growth trends inferred from tree rings. *Glob. Change Biol.* **23**, 474–484 (2017).
40. L. Duchesne *et al.*, Large apparent growth increases in boreal forests inferred from tree-rings are an artefact of sampling biases. *Sci. Rep.* **9**, 6832 (2019).
41. M. E. Dusenge, A. G. Duarte, D. A. Way, Plant carbon metabolism and climate change: Elevated CO2 and temperature impacts on photosynthesis, photorespiration and respiration. *New Phytol.* **221**, 32–49 (2019).
42. D. A. Way, R. Oren, Differential responses to changes in growth temperature between trees from different functional groups and biomes: A review and synthesis of data. *Tree Physiol.* **30**, 669–688 (2010).
43. P. E. Kauppi, M. Posch, P. Pirinen, Large impacts of climatic warming on growth of boreal forests since 1960. *PLoS One* **9**, 1–6 (2014).
44. S. M. McMahon, G. G. Parker, D. R. Miller, Evidence for a recent increase in forest growth. *Proc. Natl. Acad. Sci. U.S.A.* **107**, 3611–3615 (2010).
45. J. Barichivich *et al.*, Large-scale variations in the vegetation growing season and annual cycle of atmospheric CO2 at high northern latitudes from 1950 to 2011. *Glob. Change Biol.* **19**, 3167–3183 (2013).
46. L. T. Berner, P. S. A. Beck, A. G. Bunn, S. J. Goetz, Plant response to climate change along the forest-tundra ecotone in northeastern Siberia. *Glob. Change Biol.* **19**, 3449–3462 (2013).
47. Z. Zhu *et al.*, Greening of the Earth and its drivers. *Nat. Clim. Change* **6**, 791–795 (2016).
48. D. Schimel, B. B. Stephens, J. B. Fisher, Effect of increasing CO2 on the terrestrial carbon cycle. *Proc. Natl. Acad. Sci. U.S.A.* **112**, 436–441 (2015).
49. F. Babst *et al.*, Twentieth century redistribution in climatic drivers of global tree growth. *Sci. Adv.* **5**, eaat4313 (2019).
50. X. Zhang *et al.*, Snowmelt and early to mid-growing season water availability augment tree growth during rapid warming in southern Asian boreal forests. *Glob. Change Biol.* **25**, 3462–3471 (2019).
51. Y. Luo, H. Y. H. Chen, E. J. B. McIntire, D. W. Andison, Divergent temporal trends of net biomass change in western Canadian boreal forests. *J. Ecol.* **107**, 69–78 (2019).
52. Z. Ma *et al.*, Regional drought-induced reduction in the biomass carbon sink of Canada's boreal forests. *Proc. Natl. Acad. Sci. U.S.A.* **109**, 2423–2427 (2012).
53. S. Piao *et al.*, Evidence for a weakening relationship between interannual temperature variability and northern vegetation activity. *Nat. Commun.* **5**, 1–7 (2014).
54. C. Grossiord *et al.*, Plant responses to rising vapor pressure deficit. *New Phytol.* **226**, 1550–1566 (2020).
55. K. A. Novick *et al.*, The increasing importance of atmospheric demand for ecosystem water and carbon fluxes. *Nat. Clim. Change* **6**, 1023–1027 (2016).
56. W. Yuan *et al.*, Increased atmospheric vapor pressure deficit reduces global vegetation growth. *Sci. Adv.* **5**, 1–13 (2019).
57. L. T. Berner, B. E. Law, T. W. Hudiburg, Water availability limits tree productivity, carbon stocks, and carbon residence time in mature forests across the western US. *Biogeosciences* **14**, 365–378 (2017).
58. C. D. Allen *et al.*, A global overview of drought and heat-induced tree mortality reveals emerging climate change risks for forests. *For. Ecol. Manage.* **259**, 660–684 (2010).

59. W. R. L. Anderegg, Pervasive drought legacies in forest ecosystems and their implications for carbon cycle models. *Science.* **349**, 528–532 (2015).
60. J. S. Clark *et al.*, The impacts of increasing drought on forest dynamics, structure, and biodiversity in the United States. *Glob. Chang. Biol.* **22**, 2329–2352 (2016).
61. R. A. Hember, W. A. Kurz, N. C. Coops, Relationships between individual-tree mortality and water-balance variables indicate positive trends in water stress-induced tree mortality across North America. *Glob. Change Biol.* **23**, 1691–1710 (2017).
62. R. A. Hember *et al.*, Accelerating regrowth of temperate-maritime forests due to environmental change. *Glob. Change Biol.* **18**, 2026–2040 (2012).
63. R. R. Nemani, Climate-driven increases in global terrestrial net primary production from 1982 to 1999. *Science* **300**, 1560–1563 (2003).
64. M. P. Girardin *et al.*, Negative impacts of high temperatures on growth of black spruce forests intensify with the anticipated climate warming. *Glob. Change Biol.* **22**, 627–643 (2016).
65. N. D. Charney *et al.*, Observed forest sensitivity to climate implies large changes in 21st century North American forest growth. *Ecol. Lett.* **19**, 1119–1128 (2016).
66. A. J. Soja *et al.*, Climate-induced boreal forest change: Predictions versus current observations. *Glob. Planet. Change* **56**, 274–296 (2007).
67. P. Ciais *et al.*, Europe-wide reduction in primary productivity caused by the heat and drought in 2003. *Nature* **437**, 529–533 (2005).
68. J. A. Huang *et al.*, Radial growth response of four dominant boreal tree species to climate along a latitudinal gradient in the eastern Canadian boreal forest. *Glob. Change Biol.* **16**, 711–731 (2010).
69. M. P. Girardin *et al.*, No growth stimulation of Canada's boreal forest under half-century of combined warming and CO2 fertilization. *Proc. Natl. Acad. Sci. U.S.A.* **113**, E8406–E8414 (2016).
70. R. A. Hember, W. A. Kurz, N. C. Coops, Increasing net ecosystem biomass production of Canada's boreal and temperate forests despite decline in dry climates. *Glob. Biogeochem. Cycles* **31**, 134–158 (2017).
71. V. A. Barber, G. P. Juday, B. P. Finney, Reduced growth of Alaskan white spruce in the twentieth century from temperature-induced drought stress. *Nature* **405**, 668–673 (2000).
72. E. H. Hogg, M. Michaelian, T. I. Hook, M. E. Undershultz, Recent climatic drying leads to age-independent growth reductions of white spruce stands in western Canada. *Glob. Change Biol.* **23**, 5297–5308 (2017).
73. R. D. D'Arrigo *et al.*, Thresholds for warming-induced growth decline at elevational tree line in the Yukon Territory, Canada. *Glob. Biogeochem. Cycles* **18**, 1–7 (2004).
74. G. P. Juday, C. Alix, T. A. Grant, Spatial coherence and change of opposite white spruce temperature sensitivities on floodplains in Alaska confirms early-stage boreal biome shift. *For. Ecol. Manage.* **350**, 46–61 (2015).
75. L. Chen *et al.*, Drought explains variation in the radial growth of white spruce in western Canada. *Agric. For. Meteorol.* **233**, 133–142 (2017).
76. A. Hynes, A. Hamann, Moisture deficits limit growth of white spruce in the west-central boreal forest of North America. *For. Ecol. Manage.* **461**, 117944 (2020).
77. P. Lu, W. C. Parker, S. J. Colombo, D. A. Skeates, Temperature-induced growing season drought threatens survival and height growth of white spruce in southern Ontario, Canada. *For. Ecol. Manage.* **448**, 355–363 (2019).
78. W. A. Kurz, G. Stinson, G. J. Rampley, C. C. Dymond, E. T. Neilson, Risk of natural disturbances makes future contribution of Canada's forests to the global carbon cycle highly uncertain. *Proc. Natl. Acad. Sci. U.S.A.* **105**, 1551–1555 (2008).
79. F. Girard, S. Payette, R. Gagnon, Rapid expansion of lichen woodlands within the closed-crown boreal forest zone over the last 50 years caused by stand disturbances in eastern Canada. *J. Biogeogr.* **35**, 529–537 (2008).
80. F. Girard, S. Payette, R. Gagnon, Origin of the lichen-spruce woodland in the closed-crown forest zone of eastern Canada. *Glob. Ecol. Biogeogr.* **18**, 291–303 (2009).
81. J. P. P. Jasinski, S. Payette, The creation of alternative sTable states in the southern boreal forest, Québec, Canada. *Ecol. Monogr.* **75**, 561–583 (2005).
82. E. Whitman, M. A. Parisien, D. K. Thompson, M. D. Flannigan, Short-interval wildfire and drought overwhelm boreal forest resilience. *Sci. Rep.* **9**, 1–12 (2019).
83. D. Boucher *et al.*, Current and projected cumulative impacts of fire, drought, and insects on timber volumes across Canada. *Ecol. Appl.* **28**, 1245–1259 (2018).
84. M. Michaelian, E. H. Hogg, R. J. Hall, E. Arsenault, Massive mortality of aspen following severe drought along the southern edge of the Canadian boreal forest. *Glob. Change Biol.* **17**, 2084–2094 (2011).
85. M. H. Brice *et al.*, Moderate disturbances accelerate forest transition dynamics under climate change in the temperate–boreal ecotone of eastern North America. *Glob. Change Biol.* **26**, 4418–4435 (2020).
86. M. C. Urban *et al.*, Improving the forecast for biodiversity under climate change. *Science* **353**, 1113 (2016).
87. E. A. Burrill, A. M. Wilson, J. A. Turner, S. A. Pugh, J. Menlove, The Forest Inventory and Analysis Database: Database Description and User Guide for Phase 2 (Department of Agriculture, Forest Service, 2015).
88. Direction des inventaires forestiers du ministère des Forêts de la Faune et des Parcs, *Inventaire écoforestier placettes-échantillonspermanentes Québec* (Direction des inventaires forestiers, 5700, 4e Avenue Ouest, A108 Québec, 2018).
89. Forestry branch of Manitoba, "Manitoba Permanent Sample Plot Manual" (Forestry Branch of Manitoba, Canada, November 2008).
90. DNR, NS., "Forest inventory permanent sample plot field measurement methods and specifications" (Forest Inventory Section, Nova Scotia Department of Natural Resources, Truro Nova Scotia. Forest Inventory Report Version 1, 2002).
91. Ontario Ministry of Natural Resources and Forestry, *Ontario Growth and Yield Program PSP and PGP Reference Manual* (Ontario Ministry of Natural Resources and Forestry, Provincial Services Division, Science and Research Branch, 2016).
92. K. B. Porter, D. A. Maclean, K. P. Beaton, J. Upshall, *New Brunswick Permanent Sample Plot Database (PSPDB v1.0): User's Guide and Analysis* (Canadian Forest Service-Atlantic Forestry Center, Natural Resources Canada, 2001).
93. Public Lands, Forests Division, "Alberta permanent sample plot (PSP) field procedures manual" (Public Lands, Forests Division, 2005).
94. Saskatchewan Ministry of Environment Forest Service, "Saskathewan permanent sample plots" (Saskatchewan Ministry of Environment, Forest Service, Inventory and Planning Unit, 2011).
95. C. Peng *et al.*, A drought-induced pervasive increase in tree mortality across Canada's boreal forests. *Nat. Clim. Change* **1**, 467–471 (2011).
96. P. J. van Mantgem, Widespread increase of tree mortality rates in the Western United States. *Science* **323**, 521–524 (2009).
97. B. Bond-Lamberty *et al.*, Disturbance legacies and climate jointly drive tree growth and mortality in an intensively studied boreal forest. *Glob. Change Biol.* **20**, 216–227 (2014).
98. D. Senecal, D. Kneeshaw, C. Messier, Temporal, spatial, and structural patterns of adult trembling aspen and white spruce mortality in Quebec's boreal forest. *Can. J. For. Res.* **34**, 396–404 (2004).
99. W. R. Wykoff, N. L. Crookston, A. R. Stage, *User's Guide to the Stand Prognosis Model* (USDA For. Serv. Gen. Tech. Rep.,1982).
100. D. W. McKenney *et al.*, Customized spatial climate models for North America. *Bull. Am. Meteorol. Soc.* **92**, 1612–1622 (2011).
101. J. E. Harvey *et al.*, Tree growth influenced by warming winter climate and summer moisture availability in northern temperate forests. *Glob. Change Biol.* **26**, 2505–2518 (2020).
102. S. M. Renard, E. J. B. Mcintire, A. Fajardo, Winter conditions–not summer temperature–influence establishment of seedlings at white spruce alpine treeline in Eastern Quebec. *J. Veg. Sci.* **27**, 29–39 (2016).
103. E. H. Hogg, A. G. Barr, T. A. Black, A simple soil moisture index for representing multi-year drought impacts on aspen productivity in the western Canadian interior. *Agric. For. Meteorol.* **178–179**, 173–182 (2013).
104. T. F. Keenan *et al.*, Increase in forest water-use efficiency as atmospheric carbon dioxide concentrations rise. *Nature* **499**, 324–327 (2013).
105. S. Piao *et al.*, Evaluation of terrestrial carbon cycle models for their response to climate variability and to CO2 trends. *Glob. Chang. Biol.* **19**, 2117–2132 (2013).
106. R Core Team, *R: A Language and Environment for Statistical Computing* (R Foundation for Statistical Computing, Vienna, Austria, 2021).
107. R. J. Hijmans *et al.*, raster: Geographic Data Analysis and Modeling (R package version 3.4-13, 2021). https://cran.r-project.org/web/packages/raster/index.html.
108. J. Elith, J. R. Leathwick, T. Hastie, A working guide to boosted regression trees. *J. Anim. Ecol.* **77**, 802–813 (2008).
109. R. Caruana, A. Niculescu-Mizil, An empirical comparison of supervised learning algorithms *(Proceeding of the 23rd International Conference on Machine Learning,* 2006), 10.1145/1143844.1143865.
110. B. Greenwell, B. Boehmke, J. Cunningham, gbm: Generalized Boosted Regression Models (R package version 2.1.8, 2020). https://cran.r-project.org/web/packages/gbm/index.html
111. M. Kuhn, S. Weston, A. Williams, C. Keefer, caret: Classification and Regression Training (R package version 6.0-84, 2021). https://cran.r-project.org/web/packages/caret/.
112. B. Greenwell, pdp: Partial Dependence Plots (R package version 0.7.0, 2018). https://cran.r-project.org/web/packages/pdp/index.html
113. J. H. Friedman, B. E. Popescu, Predictive learning via rule ensembles. *Ann. Appl. Stat.* **2**, 916–954 (2008).
114. D. P. van Vuuren *et al.*, The representative concentration pathways: An overview. *Clim. Change* **109**, 5–31 (2011).
115. J. P. Brandt, The extent of the North American boreal zone. *Environ. Rev.* **17**, 101–161 (2009).
116. I. B. Marshall, P. H. Schut, M. Ballard, "A national ecological framework for Canada: Attribute data" (Agriculture and Agri-Food Canada, Research Branch, Centre for Land and Biological Resources Research, and Environment Canada, State of the Environment Directorate, Ecozone Analysis Branch, 2nd report, 1999).
117. M. C. Fitzpatrick, W. W. Hargrove, The projection of species distribution models and the problem of non-analog climate. *Biodivers. Conserv.* **18**, 2255–2261 (2009).